

# Phase transition in the modified fiber bundle model

BEOM JUN KIM(\*)

*Department of Molecular Science and Technology, Ajou University, Suwon 442-749, Korea*

PACS. 62.20.Mk – Fatigue, brittleness, fracture, and cracks.

PACS. 89.75.Hc – Networks and genealogical trees.

PACS. 05.70.Jk – Critical point phenomena.

PACS. 64.60.Fr – Equilibrium properties near critical points, critical exponents.

## Abstract. –

We extend the standard fiber bundle model (FBM) with the local load sharing in such a way that the conservation of the total load is relaxed when an isolated fiber is broken. In this modified FBM in one dimension (1D), it is revealed that the model exhibits a well-defined phase transition at a finite nonzero value of the load, which is in contrast to the standard 1D FBM. The modified FBM defined in the Watts-Strogatz network is also investigated, and found is the existences of two distinct transitions: one discontinuous and the other continuous. The effects of the long-range shortcuts are also discussed.

The fiber bundle model (FBM) was introduced to explain a variety of phenomena related with the problems of damage spread [1]. More specifically, consider a system composed of a bundle of mingled fibers exposed to a common stress along the direction of fibers. It is natural to assume that each fiber has a certain value of the capacity, or the threshold value of the load, and if the load on the fiber exceeds the capacity allowed to it, the fiber is broken. Since the broken fiber stops functioning, its neighbor fibers should carry the load which was assigned to the broken one [2]. The damage caused by the breaking of a single fiber may propagate over its local neighbors and then stop spreading. Another interesting possibility is the existence of an avalanche or a cascading failure, i.e., the original local damage spreads over the whole system, causing the complete breakdown of the total fibers. Recent blackout in the United States can also be understood as the cascading failures of power cables and power stations caused by the spread of the overload breakdowns of elements in power grid.

Recently, the subject of complex networks is the one of the most studied research area, not only for its intrinsic interest but also for its promising broad future applicability [3]. When a dynamic system is defined on a complex network, the emergent behavior may totally differ from the one on the local regular array which has been the standard arena of statistical physics. For example, the phase transitions of the Ising and the  $XY$  models on complex networks have been shown to belong to the mean-field universality class [4]. The spread of damage on networks, which is not described by the equilibrium Hamiltonian, also draws much

---

(\*) E-mail: beomjun@ajou.ac.kr

interest in relation to the epidemic spread [5] as well as the overload breakdowns of networks subject to local [6] or nonlocal [7] loads.

The fiber bundle model in this work on a general network structure is defined as follows:

1. To each vertex in the network of the size  $N$  the capacity  $c_i$  for the  $i$ th vertex is assigned at random following a given distribution function (in most cases we use the uniform distribution with  $c_i \in [0, 1]$ ).
2. The system is then exposed to a total load  $N\sigma$ , and thus each vertex should carry the same load  $\sigma_i = \sigma$  (we in this work  $\sigma = 0$  is used as an initial condition).
3. Examine the breaking condition  $\sigma_i > c_i$  for each  $i$  and if the inequality is satisfied the vertex  $i$  is broken and its load  $\sigma_i$  is equally transferred to its surviving neighbor vertices. For example, if the vertex  $i$  has  $k_i$  surviving neighbors the vertex  $j$ , which is a neighbor of  $i$ , has now new load:  $\sigma_j \rightarrow \sigma_j + \sigma_i/k_i$ . Repeat this step until there is no more breaking.
4. Increase the total load  $N\sigma \rightarrow N(\sigma + d\sigma)$ . The total load should be carried by unbroken surviving vertices, the number of which is  $N_s$ , and accordingly each vertex is assigned the new load  $\sigma_i \rightarrow \sigma_i + (N/N_s)d\sigma$ . Note that we denote the local load on the vertex  $i$  as  $\sigma_i$  while  $\sigma$  is the total load divided by  $N$ .

The above procedures are identical to the standard FBM with the local load sharing (LLS) in the literature [2]. However, our modified FBM in the present work differs as follows:

- When an isolated vertex, which has no surviving neighbor vertices, is overload broken, we assume that the load which has been carried by this vertex is not transferred to other vertices. On the other hand, in the standard FBM with LLS the load transfers via edges, not via chain of surviving vertices, and consequently the load of the broken isolated fiber can still be transferred to other (suitably defined) closely located vertices.

Our modified FBM appears to be reasonable in itself since the standard FBM assumes that the load can be transferred to vertices which are not connected to the broken vertex through a chain of *surviving* vertices. In contrast, our model allows only the load transfer across the actually existing surviving vertices. One disadvantage of our modified FBM is that the total load applied to the system is not constant in time. It might be difficult to find the actual physical realization of our model in the original context of the FBM. However, in abstract networks such as Internet one may not rule out the possibility that when an isolated vertex is broken its load does not spread to other vertices but just disappears. It should be noted that even in our modified FBM, the total load is resumed when each vertex is assigned the new load as  $\sigma_i \rightarrow \sigma_i + (N/N_s)d\sigma$  (see step 4) since the breaking of an isolated vertex also decreases  $N_s$ . Accordingly, the total load conservation condition is relaxed only during the spread of damage in step 3.

We repeat the above described procedure for our modified version of FBM and measure the ratio  $\rho \equiv N_s/N$  as a function of the load  $\sigma$  averaged over  $10^4 \sim 10^5$  different capacity distributions and different network structures. In most numerical simulations, we use  $d\sigma = 0.001$ , which has been numerically confirmed to be small enough, and network sizes are  $N = 128, 256, \dots, 524\,288$  (or from  $N = 2^7$  to  $2^{19}$ ).

We first consider the local regular one-dimensional (1D) network with the connection range  $r$ . For various values of  $r$ , including  $r = 1$  which corresponds to the usual 1D lattice, we observe the qualitatively the same behavior. In Fig. 1(a) for  $r = 2$ , it is shown that

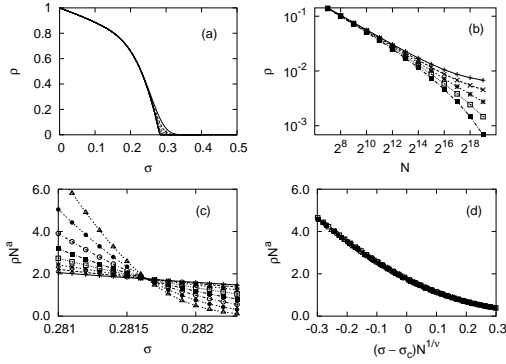


Fig. 1

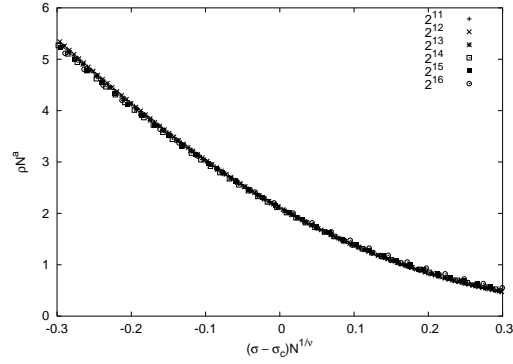


Fig. 2

Fig. 1 – The modified fiber bundle model on the 1D regular lattice with couplings up to the next nearest neighbors with the uniform distribution of the capacity  $c_i \in [0, 1]$ . (a) Density  $\rho$  of unbroken fibers versus the load  $\sigma$  for  $N = 2^7, 2^8, \dots, 2^{19}$  (from top to bottom). As  $\sigma$  is increased, the network begins to break up, resulting in  $\rho = 0$  at sufficiently large values of  $\sigma$ . (b)  $\rho$  versus  $N$  for  $\sigma = 0.2812, 0.2814, 0.2816, 0.2818$ , and  $0.2820$  (from top to bottom). Around  $\sigma \approx 0.2817$ ,  $\rho$  decays algebraically with  $N$ , manifesting the existence of the continuous phase transition. (c) Precise determination of  $\sigma_c$  from the finite-size scaling form (1). Determined are  $a = 0.50(1)$  and  $\sigma_c = 0.28165(2)$ . (Curves correspond to  $N = 2^{12}, 2^{13}, \dots, 2^{19}$ , respectively, from bottom to top on the left-hand side of the crossing point). (d) Scaling collapse of all data points in (c) through the use of the finite-size scaling (1);  $\nu = 2.0(1)$  is obtained.

Fig. 2 – The FBM on the 1D regular lattice with connections up to the next nearest neighbors with the Gaussian distribution of the capacity (the mean and the variance are fixed the same as in Fig. 1). Finite-size scaling (compare with Fig. 1 for the uniform distribution) yields  $\sigma_c = 0.27363(2)$  and critical exponents  $a = \beta/\nu = 0.50(1)$  and  $\nu = 2.0(1)$ , identical to the uniform distribution.

at a certain value of the load  $\sigma$  the ratio  $\rho$  between the number of working fibers and the total number of fibers vanishes beyond some critical value  $\sigma_c$ . As the system size  $N$  becomes larger [ $N = 2^7, 2^8, \dots, 2^{19}$  ( $= 524\ 288$ ) in Fig. 1(a)], the phase transition becomes clearer. It is interesting to note that the existence of the phase transition at nonzero  $\sigma_c$  is completely different from the well-established result of  $\sigma_c = 0$  for the standard FBM in the thermodynamic limit [2]. Simple change of the conservation law of the total load yields the dramatic change of the universality class.

We in Fig. 1 (b) show  $\rho$  as a function of  $N$  in log scales at various values of  $\sigma = 0.2812, 0.2814, 0.2816, 0.2818$ , and  $0.2820$  (from top to bottom). For  $\sigma > \sigma_c \approx 0.2817$ ,  $\rho(N)$  shows a downward curvature, implying  $\rho \rightarrow 0$  in the thermodynamic limit, while  $\rho(N)$  bends upward for  $\sigma < \sigma_c$ , suggesting that  $\rho(N)$  saturates to a finite value as  $N$  becomes larger. Separating these behaviors, there exists a well-defined  $\sigma_c$  at which  $\rho$  as a function of  $N$  decays algebraically, and the system does not possess any length scale except  $N$  at  $\sigma = \sigma_c$ . This is commonly found behavior in the system with a continuous phase transition.

For a more precise determination of  $\sigma_c$ , we use the standard finite-size scaling method with the scaling assumption:

$$\rho(\sigma, N) = N^{-a} f((\sigma - \sigma_c)N^{1/\nu}), \quad (1)$$

where  $f(x)$  is the scaling function and the exponent  $\nu$  describes the divergence of the correlation length  $\xi$  [or more generally, the correlation volume for the case when the length is ill-defined (see discussions in, e.g., Ref. [4])] near the critical point, i.e.,  $\xi \sim |\sigma - \sigma_c|^{-\nu}$ . From

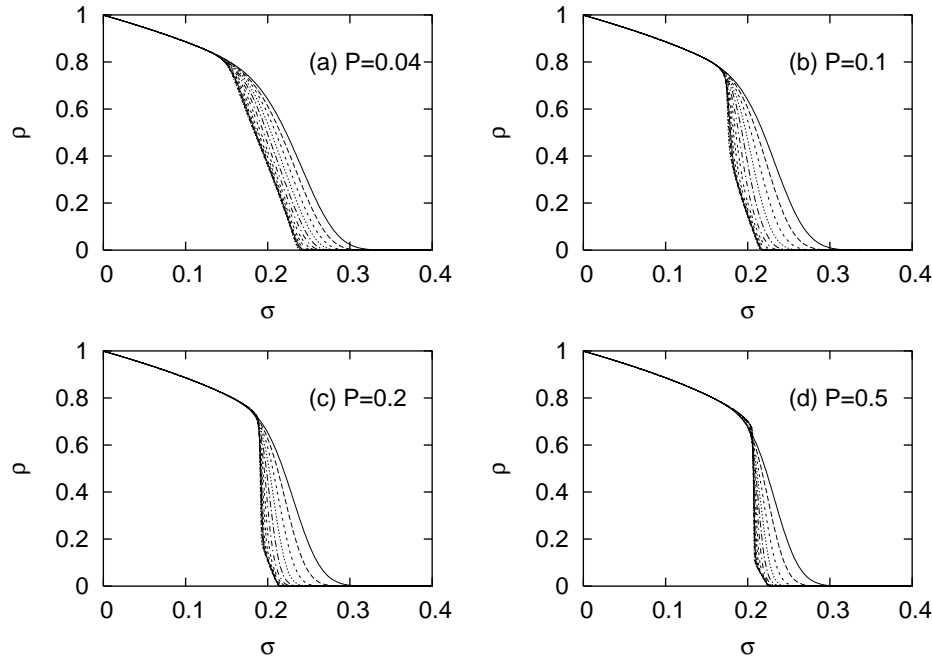


Fig. 3 – The FBM on the Watts-Strogatz small-world networks with the connection range  $r = 2$  and at various rewiring probabilities  $P =$  (a) 0.04, (b) 0.1, (c) 0.2, and (d) 0.5. Except (a), all show interesting transition behaviors: the density of working fibers  $\rho$  drops down abruptly at a certain value of the load  $\sigma_1$  and then approaches  $\rho = 0$  continuously at  $\sigma_2$ . Networks with the sizes  $N = 2^7, 2^8, \dots, 2^{19}$  (from top to bottom in each plot) and the uniform capacity distribution are used.

the definition of the critical exponent  $\beta$ ,  $\rho \sim (\sigma_c - \sigma)^\beta$  for  $\sigma < \sigma_c$  in the thermodynamic limit, we obtain the relation  $a = \beta/\nu$ . Figure 1(c) is for a precise determination of  $\sigma_c$  from the finite-size scaling (1):  $\rho N^a$  is shown to have a unique crossing point at  $\sigma = \sigma_c = 0.28165(2)$  with the exponent  $a = \beta/\nu = 0.50(1)$ . Once  $\sigma_c$  and the exponent  $a$  are determined, one can again use the finite-size scaling (1) to make the all data points in Fig. 1(c) collapse to a single smooth curve as displayed in Fig. 1(d) with the determination of  $\nu = 2.0(1)$ .

The above results of the existence of the continuous phase transition with critical exponents  $\nu \approx 2$  and  $\beta \approx 1$  is expected to be universal regardless of the detailed form of the distribution function of the capacity. We in Fig. 2 show the finite-size scaling plot for the same FBM but with the Gaussian distribution of the capacity instead. For comparisons, the same values of the mean and the variance as ones with the uniform distribution in Fig. 1 are used. Confirmed is the existence of the continuous phase transition with the identical critical exponents. Although we have not used the commonly used Weibull distribution, we believe that the universality class should be identical for the various capacity distribution functions.

We next study the FBM on the Watts-Strogatz (WS) networks, which is generated following the standard procedure in Ref. [8]. The two important parameters in the WS network are the connection range  $r$ , ( $r = 2$  is used here) and the rewiring probability  $P$  controlling the number of long-range shortcuts. As soon as  $P$  has a nonzero value, it is well-known that the network undergoes so-called small-world transition that the network diameter increases logarithmically with the network size  $N$ . In Fig. 3  $\rho$  versus  $\sigma$  is shown at  $P =$  (a) 0.04, (b)

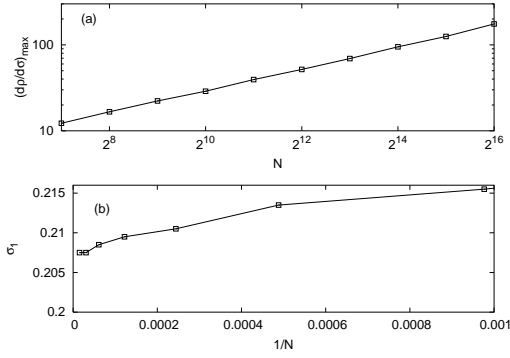


Fig. 4

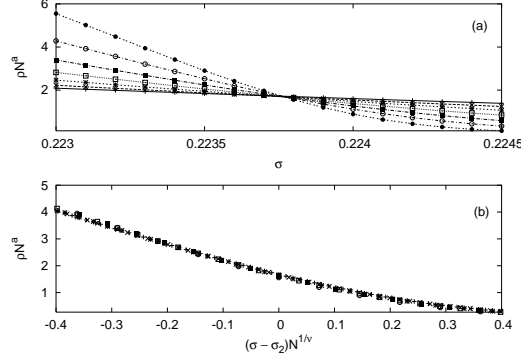


Fig. 5

Fig. 4 – The FBM on the WS network with the rewiring probability  $P = 0.5$ . (a) The maximum of the derivative of  $\rho(\sigma)$  with respect to  $\sigma$  versus the system size  $N$ . The divergence of the derivative implies the discontinuous transition nature in the thermodynamic limit.  $\sigma_1$  is defined as the value of  $\sigma$  when this maximum occurs. (b) The location  $\sigma_1$  of the derivative maximum versus  $1/N$ . In the thermodynamic limit  $\sigma_1 \approx 0.207$  is estimated.

Fig. 5 – The continuous phase transition in the FBM on the WS network with  $P = 0.5$ . (a)  $\rho N^a$  versus  $\sigma$  at various sizes  $N = 2^{13}, \dots, 2^{19}$  with  $a = 0.5$  crosses at a unique crossing point, resulting in the estimation  $\sigma_2 = 0.22376(2)$  as the critical point of the second phase transition of the continuous nature. (b) Finite-size scaling collapse (1) of data points in (a). The critical exponents  $a = \beta/\nu = 0.5, \nu = 2.0$  (and thus  $\beta = 1.0$ ) result in the scaling collapse.

0.1, (c) 0.2, and (d) 0.5. At sufficiently large values of  $P$ , it is clearly demonstrated that the system has two phase transitions at  $\sigma_1$  and  $\sigma_2$  ( $\sigma_1 < \sigma_2$ ): At  $\sigma_1$ ,  $\rho$  appears to drop abruptly to a nonzero finite value and as  $\sigma$  is further increased,  $\rho$  eventually vanishes beyond  $\sigma_2$ .

To investigate the nature of the first transition at  $\sigma_1$ , we compute  $d\rho/d\sigma$  as a function of  $\sigma$  and then measure at which value of  $\sigma$  the derivative takes the maximum value. In Fig. 4(a), the maximum value of the derivative  $(d\rho/d\sigma)_{\max}$  is plotted as a function of the system size  $N$ : The power-law divergence  $(d\rho/d\sigma)_{\max} \sim N^{0.4}$  clearly suggests that the transition nature is indeed discontinuous in the thermodynamic limit of  $N \rightarrow \infty$ . The location of the derivative maximum,  $\sigma_1$ , is displayed as a function of  $1/N$  in Fig. 4(b);  $\sigma_1 \approx 0.207$  is concluded in the thermodynamic limit. We then apply the finite-size scaling analysis to the regime where  $\rho$  approaches zero continuously (see Fig. 5). The unique crossing point in the  $\rho N^a$  versus  $\sigma$  at various  $N$  in Fig. 5(a) as well as the smooth scaling collapse in Fig. 5(b) is again observed with the identical values of critical exponents, i.e.,  $a \approx 0.5$ ,  $\nu \approx 2.0$ , and  $\beta \approx 1.0$ . It is noteworthy that the FBM on the scale-free network of Barabási and Albert (BA) [9] has shown to have a different transition nature [6], i.e., a discontinuous phase transition without the subsequent continuous transition as in the WS network considered here. Consequently, as soon as the network undergoes the global spread of the damage, no fiber survives the disaster in the BA network, while in the WS network fibers which survived the discontinuous transition are subject to the second continuous transition at a higher load.

In the context of complex networks, the size of giant component has been more frequently measured since it can detect the global breakdown of the information flow between two arbitrarily chosen vertices. In the viewpoint of the universality, the use of the different order parameters is expected to change neither the nature of the phase transition nor the values of critical exponents, which are the main interest in this work. The density of surviving fibers

in the WS network can also have a practical meaning if one considers the real fiber bundles in which most inter-fiber couplings are local while some of them are long-ranged.

Figure 6 summarizes the phase diagram obtained in the present work. There exist in general two phase transition lines separating three different phases (two unbroken phases UI and UII with  $\rho \neq 0$  and the broken phase B with  $\rho = 0$ ):  $\sigma_1$  is estimated from the maximum of  $d\rho/d\sigma$  while  $\sigma_2$  is obtained from the standard finite-size scaling analysis applied for the continuous phase transition. As the load  $\sigma$  is increased from zero, the system only suffers from locally isolated damage spreading (the phase UI in Fig. 6) until the first discontinuous transition point  $\sigma_1$  is reached. As  $\sigma$  crosses  $\sigma_1$  from below, the system undergoes abrupt change, probably in the form of the cascading failures or an avalanche, and the number of fibers still alive decays discontinuously. Interestingly, the existence of the long-range shortcuts not only makes the discontinuous transition happen, but also help the system to avoid complete disaster, i.e, the global spread of damage does not destroy all fibers in the system but there still remain a finite fraction of fibers which survived the first transition at  $\sigma_1$  (the phase UII in Fig. 6). Further increase of the load then eventually destroys all fibers resulting in the  $\rho = 0$  state (phase B in Fig. 6). At sufficiently small values of  $P$ , it appears that the system has only one phase transition which is continuous in nature: At  $P \lesssim 0.04$ , it is found that the maximum of  $d\rho/d\sigma$  and the continuous phase transition occur simultaneously. At  $P \gtrsim 0.06$ , the system starts to have well-separated two phase transitions, and the increase of  $P$  appears to make the system more strong (both  $\sigma_1$  and  $\sigma_2$  increase with  $P$  in the intermediate region).

In summary, we in this work have extended the existing model of fiber bundles in such a way that the total load conservation condition is relaxed. For a pure 1D regular network, our modified FBM has been found to show well-defined continuous phase transition at a finite nonzero value of the load  $\sigma_c$  with the critical exponents  $\beta \approx 1.0$  and  $\nu \approx 2.0$ . This is in a sharp contrast to the standard FBM where  $\sigma_c = 0$  has been confirmed in the thermodynamic limit. It has also been verified that the universality class of the phase transition does not change when different distribution function for the capacity is tried. For the Watts-Strogatz network, as the rewiring probability  $P$  is increased, the system undergoes two phase transitions at  $\sigma_1$  and  $\sigma_2$ . At  $\sigma_1$  the density  $\rho$  of working fibers decreases discontinuously to a nonzero finite value. At  $\sigma_2 (> \sigma_1)$ ,  $\rho$  approaches continuously zero, with the phase transition with the identical universality class ( $\beta \approx 1.0$  and  $\nu \approx 2.0$ ). The roles played by the existence of long-range shortcuts have been shown to be two-fold: On the one hand, long-range shortcuts make the fiber breaking transition abrupt, helping the damage spread across the system more easily. On the other hand, the long-range shortcuts prohibit the system from being completely destroyed, and even after the global propagation of damage (at  $\sigma_1$ ), there still remain a finite fraction of fibers still working.

The author thanks D.H. Kim for useful discussions. This work has been supported by the Korea Science and Engineering Foundation through Grant No. R14-2002-062-01000-0 and Hwang-Pil-Sang research fund in Ajou University. Numerical works have been performed on the computer cluster Iceberg at Ajou University.

## REFERENCES

- [1] Daniels H.E., Proc. R. Soc. London A, **183** (1945) 405; Coleman B.D., J. Appl. Phys., **28** (1957) 1058; Sen P.K., J. Appl. Proc., **10** (1973) 586. Phoenix S.L. and Taylor H.M., Adv. Appl. Prob., **5** (1973) 200; Hemmer P.C. and Hansen A., J. Appl. Mech., **59** (1992) 909; Sornette D., J. Phys. A, **22** (1989) L243; J. Phys. I (France), **2** (1992) 2089.
- [2] Smith R.L., Proc. R. Soc. London A, **372** (1980) 539; Harlow D.G. and Phoenix S.L., Int. J. Fracture, **17** (1981) 601; Gómez J.B., Iñiguez D. and Pacheco A.F., Phys. Rev. Lett., **71** (1993)

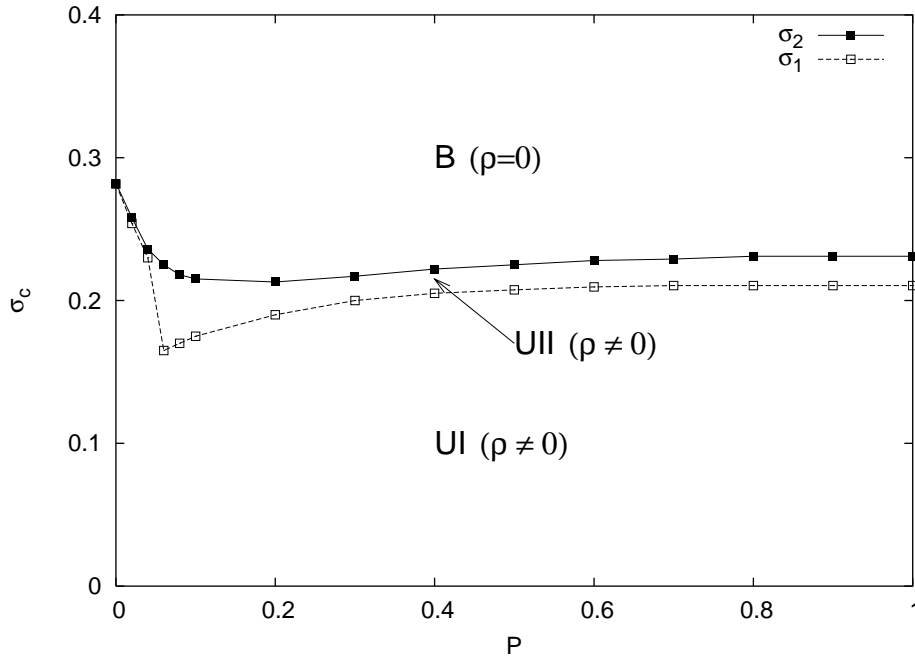


Fig. 6 – Phase diagram of the FBM on the WS network with the connection range  $r = 2$ . The points (filled squares) on the full line are obtained from the finite-size scaling analysis for the continuous phase transition (see Fig. 5) and the points (empty squares) on the dotted line are from the maximum position of  $dp/d\sigma$  extrapolated to  $N \rightarrow \infty$  (see Fig. 4). There exist three phases: two unbroken phases with  $\rho \neq 0$  (UI and UII), and completely broken phase with  $\rho = 0$  (B). In UI, most fibers are still working with higher value of  $\rho \gtrsim 0.7$ , while in UII only small fraction (but still nonzero) of fibers hold together to endure the external load. The transition between UI and UII is discontinuous while between UII and B the nature of the transition is continuous. For sufficiently small values of  $P (\lesssim 0.04)$ , it appears that there exists only one transition from UI to B.

380; Duxbury P.M and Leath P.L., Phys. Rev. B, **49** (1994) 12676; Vázquez-Prada, Gómez, Moreno Y. and Pacheco A.F., Phys. Rev. E, **60** (1999) 2581; Hidalgo R.C., Moreno Y. Kun F. and Herrmann H.J., Phys. Rev. E, **65** (2002) 046148; Pradhan S. and Chakrabarti, Int. J. Mod. Phys. B, **17** (2003) 5565.

- [3] For general reviews, see, e.g., Watts D.J., *Small Worlds* (Princeton University Press, Princeton, 1999); Albert R. and Barabási A.-L., Rev. Mod. Phys., **74**, (2002) 47; Dorogovtsev S.N. and Mendes J.F.F., *Evolution of Networks* (Oxford University Press Inc., New York, 2003).
- [4] Gitterman M., J. Phys. A: Math. Gen., **33** (2000) 8373; Barrat A. and Weigt M., Eur. Phys. J. B, **13** (2000) 547; Hong H., Kim B.J. and M.Y. Choi, *ibid.*, **66** (2002) 018101; Kim B.J., Hong H., Holme P., Jeon G.S., Minnhagen P. and Choi M.Y., Phys. Rev. E, **64** (2001) 056135.
- [5] Kuperman M. and Abramson G., Phys. Rev. Lett., **86** (2001) 2909; Moore C. and Newman M.E.J., Phys. Rev. E, **61** (2000) 5678 (2000); Pastor-Satorras R. and Vespignani A., Phys. Rev. Lett., **86** (2001) 3200; Moreno Y. and Vázquez A., Eur. Phys. J. B, **31** (2003) 265.
- [6] Moreno Y., Gómez J.B. and Pacheco A.F., Europhys. Lett., **58** (2002) 630 (2002).
- [7] Holme P. and Kim B.J., Phys. Rev. E, **65** (2002) 066109.
- [8] Watts D.J. and Strogatz S.H., Nature (London), **393** (1998) 440.
- [9] Barabási A.-L. and Albert R., Science, **286** (1999) 509; Barabási A.-L., Albert R. and Jeong H., Physica A, **272** (1999) 173.